

Article

Pseudomonas indica-Mediated Silver Nanoparticles: Antifungal and Antioxidant Biogenic Tool for Suppressing Mucormycosis Fungi

Salem S. Salem ¹, Omar M. Ali ^{2,*}, Ahmed M. Reyad ^{3,4}, Kamel A. Abd-Elsalam ^{5,*}
and Amr H. Hashem ^{1,*}

¹ Department of Botany and Microbiology, Faculty of Science, Al-Azhar University, Nasr City, Cairo 11884, Egypt; salemsalahsalem@azhar.edu.eg

² Department of Chemistry, Turabah University College, Turabah Branch, Taif University, Taif 21944, Saudi Arabia

³ Biology Department, Faculty of Science, Jazan University, Jazan 82817, Saudi Arabia; areyadegy@yahoo.com

⁴ Botany and Microbiology Department, Faculty of Science, Beni-Suef University, Beni-Suef 62511, Egypt

⁵ Plant Pathology Research Institute, Agricultural Research Centre, Giza 12619, Egypt

* Correspondence: om.ali@tu.edu.sa (O.M.A.); kamelabdsalam@gmail.com (K.A.A.-E.); amr.hosny86@azhar.edu.eg (A.H.H.)

Abstract: Mucormycosis is considered one of the most dangerous invasive fungal diseases. In this study, a facile, green and eco-friendly method was used to biosynthesize silver nanoparticles (AgNPs) using *Pseudomonas indica* S. Azhar, to combat fungi causing mucormycosis. The biosynthesis of AgNPs was validated by a progressive shift in the color of *P. indica* filtrate from colorless to brown, as well as the identification of a distinctive absorption peak at 420 nm using UV-vis spectroscopy. Fourier-transform infrared spectroscopy (FTIR) results indicated the existence of bioactive chemicals that are responsible for AgNP production. AgNPs with particle sizes ranging from 2.4 to 53.5 nm were discovered using transmission electron microscopy (TEM). Pattern peaks corresponding to the 111, 200, 220, 311, and 222 planes, which corresponded to face-centered cubic forms of metallic silver, were also discovered using X-ray diffraction (XRD). Moreover, antifungal activity measurements of biosynthesized AgNPs against *Rhizopus Microsporus*, *Mucor racemosus*, and *Syncephalastrum racemosum* were carried out. Results of antifungal activity analysis revealed that the biosynthesized AgNPs exhibited outstanding antifungal activity against all tested fungi at a concentration of 400 µg/mL, where minimum inhibitory concentrations (MIC) were 50, 50, and 100 µg/mL toward *R. microsporus*, *S. racemosum*, and *M. racemosus* respectively. In addition, the biosynthesized AgNPs revealed antioxidant activity, where IC₅₀ was 31 µg/mL when compared to ascorbic acid (0.79 µg/mL). Furthermore, the biosynthesized AgNPs showed no cytotoxicity on the Vero normal cell line. In conclusion, the biosynthesized AgNPs in this study can be used as effective antifungals with safe use, particularly for fungi causing mucormycosis.

Keywords: silver nanoparticles; green biosynthesis; antifungal activity; mucormycosis; antioxidant activity



Citation: Salem, S.S.; Ali, O.M.; Reyad, A.M.; Abd-Elsalam, K.A.; Hashem, A.H. *Pseudomonas indica*-Mediated Silver Nanoparticles: Antifungal and Antioxidant Biogenic Tool for Suppressing Mucormycosis Fungi. *J. Fungi* **2022**, *8*, 126. <https://doi.org/10.3390/jof8020126>

Academic Editor: Vincent Bruno

Received: 14 January 2022

Accepted: 25 January 2022

Published: 27 January 2022

Publisher's Note: MDPI stays neutral with regard to jurisdictional claims in published maps and institutional affiliations.



Copyright: © 2022 by the authors. Licensee MDPI, Basel, Switzerland. This article is an open access article distributed under the terms and conditions of the Creative Commons Attribution (CC BY) license (<https://creativecommons.org/licenses/by/4.0/>).

1. Introduction

More than 1.2 billion people are infected by pathogenic fungus each year, resulting in at least 1.7 million fatalities [1,2]. Fungal pathogens now outnumber drug-resistant *Mycobacterium tuberculosis* in terms of mortality, and they even outnumber malaria [3]. Mucormycosis is one of the most dangerous fungal diseases for humans. Mucormycosis is a disease caused by a group of fungi called mucormycetes, which includes various genera such as *Rhizopus*, *Mucor*, *Syncephalastrum*, *Absidia*, and *Cunninghamella* [4,5]. These fungi invade people with a history of diabetes, stem cell transplants, cancer, injection drug use,

skin injury due to surgery, burns, or wounds [6–8]. Mucormycosis is a serious infection and needs to be treated with prescription antifungal medicine, usually amphotericin B, posaconazole, or isavuconazole [9]. The increasing usage of antifungal medications has resulted in the emergence of fungal strains such as *Candida albicans* [10], *Lichtheimia corymbifera*, *R. microsporus*, *R. arrhizus*, and *M. circinelloids* that are resistant to the majority of antifungal treatments [11,12]. Most harmful fungi, similar to bacteria, have recently developed antibiotic resistance. To combat drug-resistant fungus, novel antifungal medicines based on current biotechnology must be investigated.

Nanoparticles (NPs) are a diverse class of materials that appeal to several researchers due to their tiny size (1–100 nm), exceptional properties, large surface area, enhanced reactivity, capacity to access the body easily, and multiple uses in modern science, including the industrial and medicinal sciences [13–20]. Selenium, silver, copper, magnesium, zinc, and titanium are some of the nanoparticles that have been reported [21–30]. AgNPs are widely utilized nanoparticles in numerous sectors of study, such as optical devices, ophthalmology, pharmaceutical, and the health sciences, for the creation of drug carriers, chemotherapeutic, nano-sensors, gene therapy, and other applications [31–36]. AgNPs have been shown to exhibit high antibacterial, anti-inflammatory, antibiofilm, and anticancer characteristics, with the antimicrobial capabilities of AgNPs being used to prevent infection against harmful microorganisms, such as eukaryotic microorganisms, bacteria, and viruses [37–40]. AgNPs are widely used in the biomedical control of diseases such as candidiasis [35] and aspergillosis [41] [42,43]. The efficacy of AgNPs as antimicrobial against microorganisms may be due to their link with enzymes, reactive oxygen species (ROS) levels, and changing structure contents that alter the membrane integrity and morphology [44–46]. Because of their antibacterial, anti-inflammatory, antibiofilm, anticoagulant, and anticancer properties, AgNPs are becoming a popular choice in the medical and biological fields [22,47,48]. Physical and chemical approaches for the synthesis of NPs are extensively utilized, but they have several downsides, such as the usage of high energy or dangerous chemicals, their high cost, and the generation of vast volumes of toxic byproducts that pollute the environment [49]. To overcome the constraints of physical and chemical procedures, low-cost, ecofriendly, simple, and nontoxic approaches that eliminate the use of hazardous and pricey solvents are required for metallic NPs manufacturing [50]. Biological synthesis of metal nanoparticles should be stable, biologically safe and ecofriendly [51–55]. Bacteria are one of the most significant groups of microorganisms, since they are employed in bioprocessing, enzyme manufacturing, acid generation, and nanotechnology, among other uses [56–58]. Microbial variety may be found in abundance in soil, and these microorganisms can be harnessed to benefit humans. Soil bacteria also require a low cost and low-nutrient medium for growth, making them an ideal option for use [47]. In this work, the bacterial strain *P. indica* S. Azhar was isolated from a soil sample and utilized to synthesize AgNPs in a simple, quick, and environmentally friendly manner. AgNPs were investigated and characterized by UV-vis, Ft-IR, TEM, and XRD. An attempt was made to investigate the antifungal and antioxidant activities of AgNPs against three mold strains (*Rhizopus microsporus*, *Mucor racemosus*, and *Syncephalastrum racemosum*) which cause mucormycosis in vitro.

2. Materials and Methods

2.1. Isolation and Identification of Strain S. Azhar

The bacterial strain *P. indica* S. Azhar was isolated from a soil sample collected from the garden of the Faculty of Science, Al-Azhar University, Cairo, Egypt. For the isolation of bacterial strains, nutrient agar medium was used. The 16S rRNA gene sequencing for bacteria was used to identify it genetically. The improved approach was used to extract bacterial genomic DNA. Single colonies were taken from agar plates and suspended in sterile deionized water in 50 µL. The cell suspension was then incubated in a water bath for 10 min at 97 °C before being centrifuged for 10 min at 15,000 rpm to separate the DNA-containing cell lysate. Using a genomic DNA template and two universal primers, PCR was utilized to amplify the 16S rRNA gene. The primers 27-f (5-AGAGTTTGATCCTGGCTCAG-3)

and 1492-r were utilized (5-GGTTACCTTGTTACGACTT-3). Amounts of $1\times$ PCR buffer, 0.5 mM $MgCl_2$, 2.5 U Taq-polymerase (QIAGEN, Hilden, Germany), 0.25 mM dNTP, 0.5 M of each primer, and $1\ \mu L$ of isolated genomic DNA were added into the PCR mixture (50 μL). Sigma Scientific Services Company (Cairo, Egypt) used a Thermal Cycler to execute the PCR, which included a 3 min hot start at $94\ ^\circ C$, 30 cycles at $94\ ^\circ C$ for 30 s, $55\ ^\circ C$ for 30 s, and $72\ ^\circ C$ for 1 min, and 10 min of gene extension at $72\ ^\circ C$. GATC Company used an ABI 3730x1 DNA sequencer to evaluate the sequencing (Ebersberg, Germany). Using the NCBI BLAST software, the acquired sequences were compared to those in the GenBank database. The bootstrap technique was used to create the phylogenetic tree.

2.2. Extracellular Biosynthesis of AgNPs

2.2.1. Bacterial Filtrate Preparation

P. indica cells were suspended in nutrient and injected in broth media for fermentation at $36 \pm 2\ ^\circ C$ for 48 h in an orbital shaker (120 rpm). The biomass was collected using filter paper No. 1 and rinsed in sterilized distilled water to eliminate any medium components before being suspended in 100 mL distilled water. At $34 \pm 2\ ^\circ C$, the mixture was stirred for 24 h. Finally, the biomass filtrate was produced by passing it through Whatman filter paper No. 1 and centrifuging it for 5 min at 2000 rpm to sediment any remaining cell debris. The supernatant was used for AgNPs biosynthesis.

2.2.2. Biosynthesis of AgNPs by Biomass Filtrate

For the production of AgNPs, the previously prepared bacterial biomass filtrate of *P. indica* was employed as follows: in a 250 mL flask, 1 mM silver nitrate was combined with 100 mL biomass filtrate and incubated at $36 \pm 2\ ^\circ C$ for 24 h, and agitated at 150 rpm, as shown in Figure 1. Negative controls (cell filtrate) were also run along with the experiment.

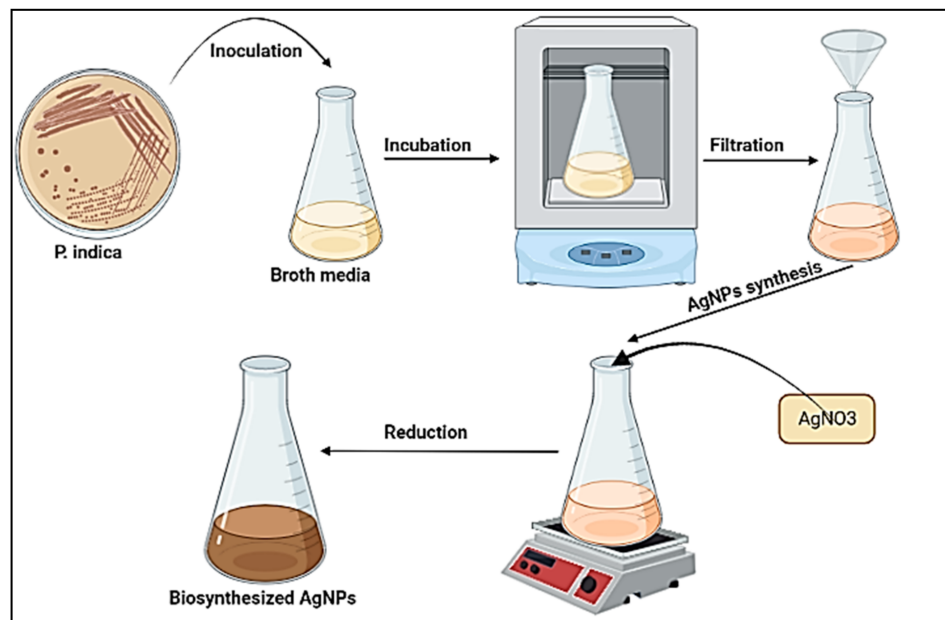


Figure 1. Process for the biosynthesis of AgNPs.

2.3. Characterization of AgNPs

The absorption characteristics of biogenically produced AgNPs were evaluated using UV-vis spectrophotometry (JENWAY 6305 Spectrophotometer, UK). Quartz cuvettes were used to investigate solutions containing AgNPs in the wavelength range 200–800 nm. Allocating the peak in the region of 400 to 500 nm indicated the existence of AgNPs. In a mortar, a known weight of AgNPs, 1 mg, was ground with dry 2.5 mg of KBr. The powder was then placed in a 2 mm micro-cup with a 2 mm internal diameter and loaded

onto a FT-IR set at $26\text{ }^{\circ}\text{C} \pm 1\text{ }^{\circ}\text{C}$. The sample was scanned using infra-red in the range of $400\text{--}4000\text{ cm}^{-1}$, utilizing Fourier transform-infrared spectrometry. To determine the size and form of nanoparticles, TEM (JEOL 1010, Tokyo, Japan) was used to characterize AgNPs. Drop-coating the AgNPs solution onto the carbon-coated copper grid and loading it onto a specimen holder were used to produce the sample. The sizes and shapes of AgNPs were validated using TEM micrographs. Stress analysis, residual-austenite quantitation, crystallite size/lattice, crystallite calculation, and materials analysis by overlaid X-ray diffraction patterns with a Shimadzu apparatus, using a nickel filter and Cu-K α target (Shimadzu-Scientific Instruments (SSI), Kyoto, Japan), were obtained with the XRD 6000 series. The average crystallite size of AgNPs can also be measured utilizing the Debye-scherrer equation: $D = k\lambda/\beta \text{ Cos } \theta$.

2.4. Antifungal Activity

Some genera of the Mucorales group were used for evaluation of the biosynthesized AgNPs as antifungal agent. *Rhizopus microsporus* (Accession no. MK623262.1), *Mucor racemosus* (Accession no. MG547571.1), and *Syncephalastrum racemosum* (Accession no. MK621186.1) were obtained from the Mycology Lab., Faculty of Science, Al-Azhar University. These three fungal strains were inoculated on malt extract agar (MEA) (Oxoid) plates, incubated for 3–5 days at $28 \pm 2\text{ }^{\circ}\text{C}$, and then stored at $4\text{ }^{\circ}\text{C}$ for future use [59–62]. Antifungal activity of AgNPs at $400\text{ }\mu\text{g/mL}$ were tested according to methods used by Dacroy et al. [5] with minor modifications. Briefly, $100\text{ }\mu\text{L}$ of AgNPs were added to plates, prepared previously on MEA media streaked with purified fungal strains (10^7 spores/mL). The plates were incubated for 2–3 days at $30 \pm 2\text{ }^{\circ}\text{C}$. Minimum inhibitory concentration of AgNPs toward all tested fungal strains was assessed using the broth microdilution technique, according to the standard EUCAST methodology [63].

2.5. Antioxidant Activity

1,1-Diphenyl-2-picrylhydrazyl (DPPH) free radical-scavenging activity of the biosynthesized AgNPs was determined according to the method used by Khalil et al. [64], with minor modifications. Different concentrations of biosynthesized AgNPs ($400\text{--}0.78\text{ }\mu\text{g/mL}$) were used to determine the antioxidant activity. The DPPH solution ($800\text{ }\mu\text{L}$) was combined with $200\text{ }\mu\text{L}$ of the sample concentration and maintained at $25\text{ }^{\circ}\text{C}$ in the dark for 30 min. After that, the absorbance was measured at 517 nm against a blank after centrifugation for 5 min at $13,000\text{ rpm}$. The standard for this experiment was ascorbic acid. The following formula was used to determine antioxidant activity:

$$\text{Antioxidant activity (\%)} = \frac{\text{Control absorbance} - \text{Sample absorbance}}{\text{Control absorbance}} \times 100$$

2.6. In-Vitro Cytotoxicity

The cytotoxicity of AgNPs, at concentrations ranging from 31.25 to $1000\text{ }\mu\text{g/mL}$, was tested against normal Vero cell lines obtained from ATCC using the MTT procedure [65] with minor modifications. As mentioned in Equation (1), the viability percentages were computed as follows:

$$\text{Viability \%} = \frac{\text{Test OD}}{\text{Control OD}} \times 100 \quad (1)$$

3. Results

3.1. Bacterial Strain Identification

Isolate S. Azhar's 16S rRNA gene sequence was 1140 bp , and the sequence was uploaded to NCBI (accession number MW820210). Strain S. Azhar has the greatest sequence similarity to *P. indica*, based on the 16S rRNA gene sequencing analysis. A neighbor-joining tree phylogenetic study further revealed that strain S. Azhar belonged to the *Pseudomonas* genus (Figure 2).

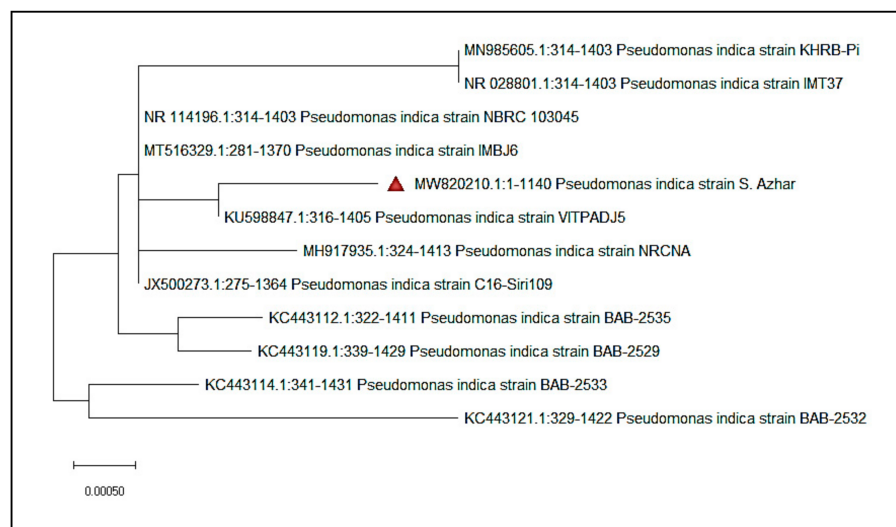


Figure 2. A neighbor-joining (NJ) tree based on 16S rRNA gene sequence analysis was used to show the phylogenetic relationships of the isolated strain S. Azhar with comparable type strains.

3.2. Synthesis and Characterization of AgNPs

In this study, biomass filtrate of *P. indica* was incubated with 1 mM AgNO₃ for 24 h in dark conditions. Appearance of brown color after contacting of the filtrate of *P. indica* S. Azhar with precursor (AgNO₃) at the reaction completion indicated AgNPs' formation; maximum absorbance peaks at 420 nm were seen in the UV-vis spectral analysis, which might correlate to spherical AgNPs, as seen in Figure 3A. Surface plasmon resonance (SPR) excitation might be responsible for the color alteration. After calcination, AgNPs were obtained as a black powder. The functional groups of those found in AgNPs were characterized using FT-IR analysis. As seen in Figure 3B. The occurrence of functional assemblies of biomolecules was discovered using FTIR wavelengths of 400 to 4000 cm⁻¹. Ten prominent peaks in the FTIR spectra of biosynthesized AgNPs were found at 474.4, 617.1, 1110.8, 1382.7, 1617.9, 1637.2, 2032.6, 2921.6, 3235.9 and 3415.3 cm⁻¹ (Figure 3B). The peaks at 3235.9 and 3415.3 cm⁻¹ correspond to the alcohol O–H stretching group or the secondary amine N–H stretching group. NH stretching of the protein's amide I band is shown by the bands at 1637.2 and 1617.9 cm⁻¹. Alkyne stretch bands are represented by the peaks at 2032.6 and 2921.6 cm⁻¹. Furthermore, the bands seen at 1382.7 and 1110.8 cm⁻¹ might be attributed to aromatic and aliphatic amine C–N stretching vibrations. Finally, the peaks at 617.1 and 474.4 cm⁻¹ correspond to the bending of alkene (C=H) groups. As a result, the current work reveals that proteins or bacterial extracts attach quickly to AgNPs via the proteins' free amino or carboxyl groups; moreover, the acquired form of NPs changes as the protein binding with AgNPs varies.

The most effective approach for identifying morphological features, such as the size and form, of biosynthesized AgNPs is TEM examination. Figure 4 reveals the effective manufacture of spherical AgNPs using metabolites found in *P. indica* S. Azhar's filtrate, with typical sizes ranging from 2.4 to 53.5 nm. Furthermore, the biologically produced nanoparticles were evenly diffused, with no aggregation or morphological discrepancy.

XRD based AgNPs characterization exhibited five peaks at 2θ values: 38.2°, 44.46°, 64.22°, 77.52°, and 81.22°, which were assigned to planes 111, 200, 220, 311, and 222, respectively for AgNPs Figure 5A. The average sizes of crystallite Ag- particles were calculated using Scherrer's equation. In this context, the size of Ag particles ranged between 8 to 80 nm, which were the outputs from the analysis of the equation. In line with our clarification of the results, we reported the successful fabrication of crystallite, monoclinic-phase AgNPs at the same XRD diffraction planes utilizing metabolites of *P. indica* S. Azhar.

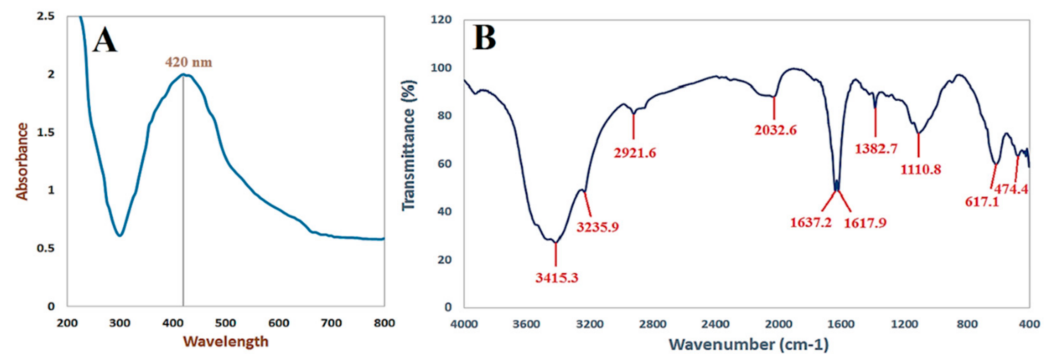


Figure 3. UV-Vis spectrophotometer (A) and FT-IR spectra (B) of AgNPs synthesized by *P. indica* S. Azhar.

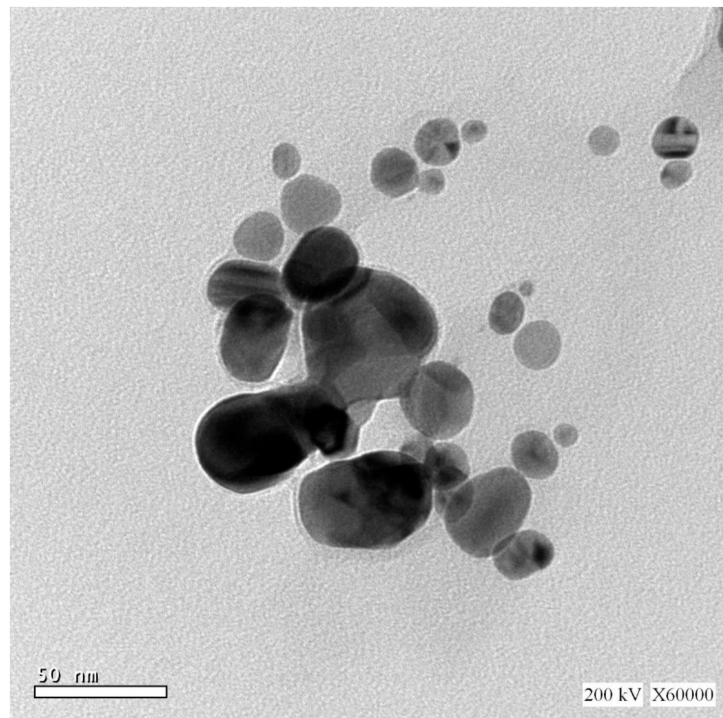


Figure 4. TEM image of AgNPs synthesized by of *P. indica* S. Azhar.

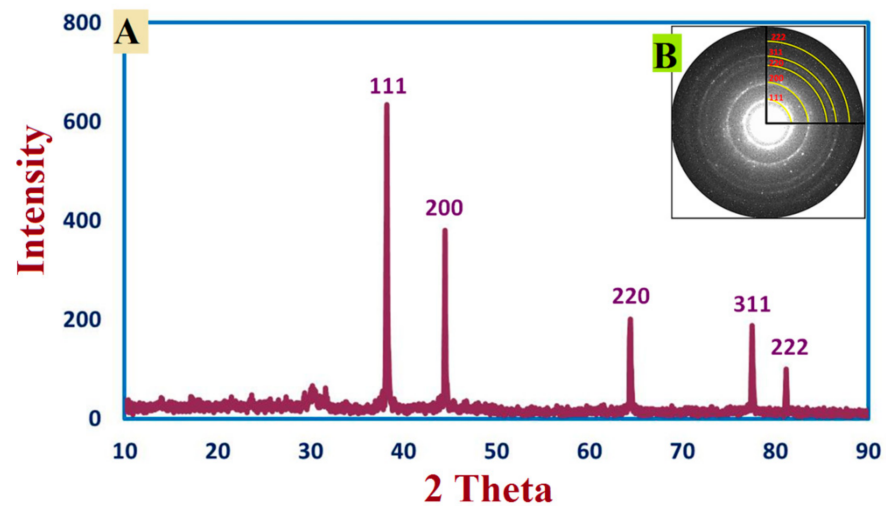


Figure 5. XRD pattern (A) and SAED pattern (B) of biosynthesized AgNPs.

3.3. Antifungal Activity

In this study, the antifungal activity of biosynthesized AgNPs against *R. microsporus*, *M. racemosus* and *S. racemosum* was carried out as shown in Figure 6. Results illustrated that the biosynthesized AgNPs exhibited outstanding antifungal activity against all tested fungal strains. Moreover, the antifungal activity was the highest toward *R. microsporus*, where the inhibition zone was 38 mm at a concentration of 400 $\mu\text{g}/\text{mL}$ of AgNPs. Furthermore, AgNPs at concentration 400 $\mu\text{g}/\text{mL}$ exhibited potential antifungal activity against *S. racemosum*, but this was lower than for *R. microsporus*, where the inhibition zone was 24 mm. On the other hand, the antifungal activity was the lowest toward *M. racemosus* where the inhibition zone was 19 mm, as shown in Figure 6A. Moreover, the MIC of AgNPs was assessed using the broth microdilution method against all tested fungal strains. Results revealed that the MIC of AgNPs was in the range of 50–100 $\mu\text{g}/\text{mL}$ according to the fungal strain, where MIC was 50 $\mu\text{g}/\text{mL}$ toward *R. microspores* and *S. racemosum*, while it was 100 $\mu\text{g}/\text{mL}$ against *M. racemosus*, as shown in Figure 6B.

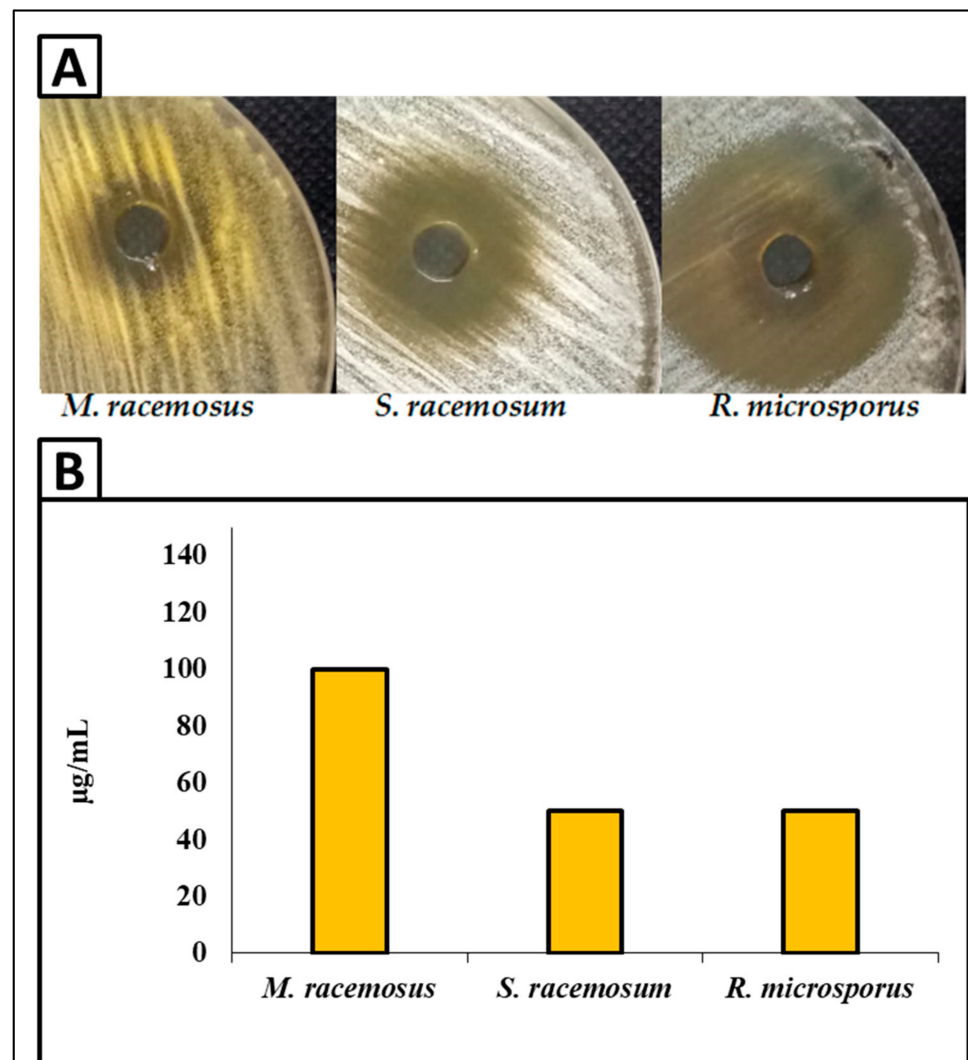


Figure 6. Antifungal activity of AgNPs at 400 $\mu\text{g}/\text{mL}$ using the agar well diffusion method (A) and the MIC of AgNPs using the broth microdilution method (B) toward *R. microsporus*, *S. racemosum*, and *M. racemosus*.

3.4. Antioxidant Activity

In this study, the antioxidant activity of AgNPs at different concentration (400–0.78 $\mu\text{g}/\text{mL}$) was evaluated using the DPPH method as shown in Figure 7. Results showed that AgNPs exhibited antioxidant activity, where the IC_{50} was 31 $\mu\text{g}/\text{mL}$ when compared to ascorbic acid (0.79 $\mu\text{g}/\text{mL}$). In addition, antioxidant activity at 400, 200, 100, and 50 $\mu\text{g}/\text{mL}$ were 96%, 86.6%, 72%, and 59.6%, respectively, and antioxidant activity decreased with decreasing concentrations, where the activity was 1% at 0.78 $\mu\text{g}/\text{mL}$. This suggests the possible application of AgNPs as an alternative antioxidant in the treatment of diseases that are caused due to free radicals.

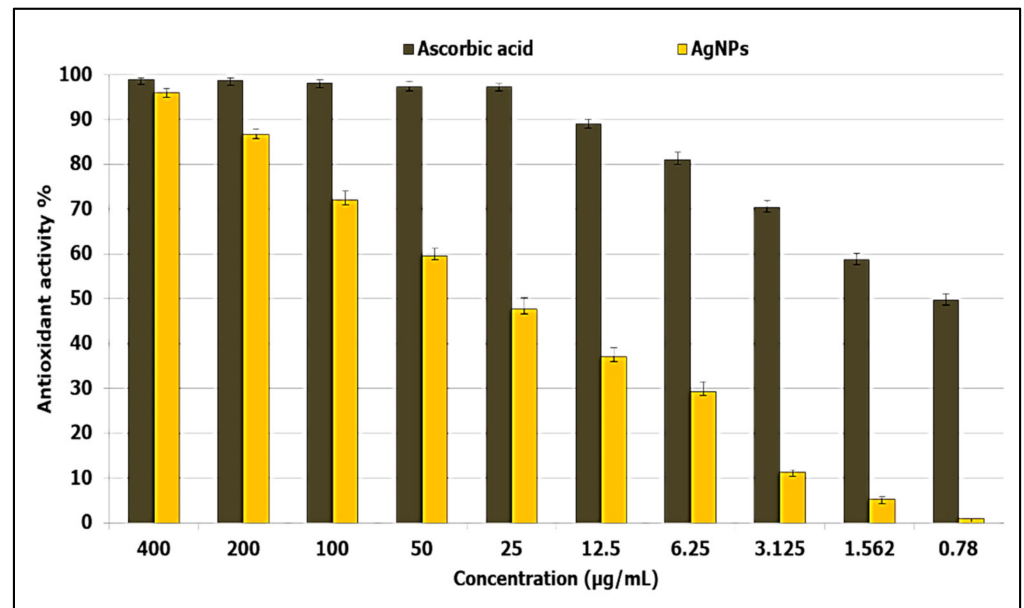


Figure 7. Antioxidant activity of AgNPs at different concentrations using DPPH method.

3.5. Cytotoxicity

Evaluation of the cytotoxicity of compounds in human normal cell lines is considered the first step to detect their safety [64]. Cytotoxicity of AgNPs at different concentrations was tested against the Vero cell line CCL-81, as illustrated in Figure 8. Results revealed that the IC_{50} of the biosynthesized AgNPs was 132.2 $\mu\text{g}/\text{mL}$, and the cell viability of Vero cells at two concentrations, 31.25 and 62.6 $\mu\text{g}/\text{mL}$, was 99% and 98%, respectively, which confirmed no cytotoxic effect of AgNPs at these two concentrations. In general, if the IC_{50} is ≥ 90 $\mu\text{g}/\text{mL}$, the material is classified as non-cytotoxic [66]. Therefore, this confirmed that the biosynthesized AgNPs are safe to use.

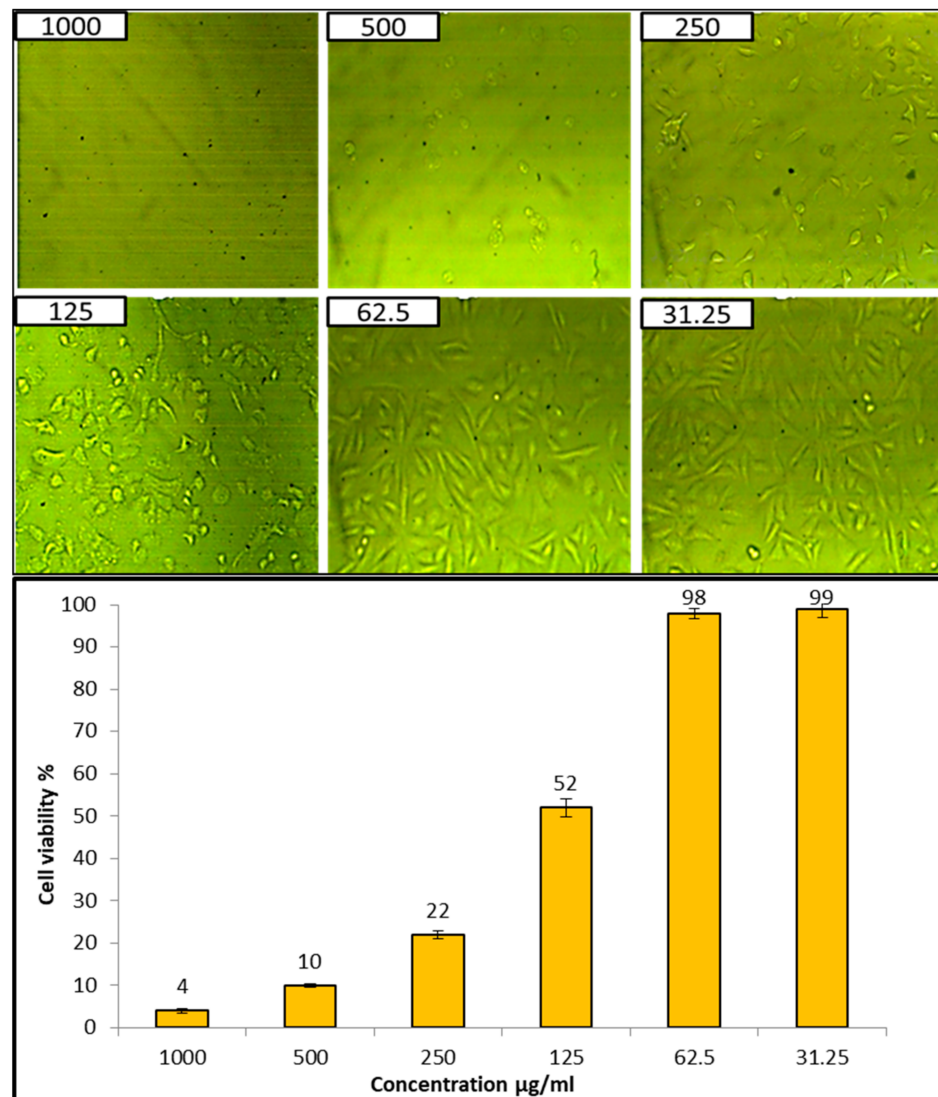


Figure 8. Cytotoxicity of AgNPs on Vero cell line.

4. Discussion

Green biosynthesis of AgNPs has risen in prominence as a potential alternative to chemical and physical techniques. Metabolites secreted by *P. indica* S. Azhar are effective in the formation of AgNPs, besides stabilizing the formed NPs. *P. indica* S. Azhar filtrate was utilized as a bio-reactor for the formation of AgNPs through harnessing bioactive macromolecules that are secreted from it. *P. indica* nanoparticles are currently in the early phases of development. *P. indica*-derived biogenic AgNPs are more appealing and less hazardous to the environment than other approaches. The proteins or enzymes involved in cell-free filtrates of *P. indica* that change nitrate to nitrite, and then reduced silver ions to silver in the metallic form, may be responsible for the synthesis of AgNPs. The absorbance peak at 420 nm in the UV-visible spectrum corresponded to the typical band of AgNPs generated by the *P. indica* cell free filtrate. The absorption peak at around 400–450 nm is attributed to AgNPs surface plasmon resonance, confirming the production of AgNPs [67]. Similarly, Alsharif et al. [68] observed that AgNPs generated by *Bacillus cereus* presented a single symmetric maximum at wavelength 420 nm, which is linked to spherical structure. The capping of biosynthesized AgNPs was discovered using Fourier transform-infrared spectroscopy. The FT-IR spectral analysis of AgNPs revealed N–H aliphatic amino group peaks at 3415.3 and 3235.9 cm^{-1} , whereas the $-\text{CH}_2$ group is indicated by the peak at

2921.6 cm^{-1} [69]. The (OH) stretch of the carboxyl group is shown by the spectrum peak at 2032.6 cm^{-1} . The binding of the amide I band of protein with the (N–H) stretch is associated with the peaks at 1637.2 and 1617.9 cm^{-1} [22]. The C–H and C–O stretching bands may be recognized at 1382.9 and 1110.8 cm^{-1} , respectively [47]. The relationship between Ag and physiologically active chemicals that are responsible for the production and stability of AgNPs as capping agents was investigated using FTIR. The infrared area of the spectrum is designated by the carboxylic acid group (CHOO–), obtained with an amine (NH₂) in the amino acid of proteins [70]. The most efficient approach for identifying morphological features, such as the size and form of produced AgNPs, is TEM examination. According to TEM data, the biosynthesized AgNPs had a spherical form with a size range of 2.4 to 53.5 nm. According to a previous study, researchers successfully formed spherical AgNPs with a size range of 6–50 nm using TEM, as seen in Alsharif et al. [68]. Other reports showed a difference in the shape and size of AgNPs biologically formed by bacteria [71,72]. The size range of AgNPs generated by *B. licheniformis* filtrate during incubation with 1 and 3 mM AgNO₃ was (3–130 nm) and (45–170 nm), respectively, according to Sarangadharan and Nallusamy [73]. When the biomass of *B. licheniformis* was incubated with 1 mM AgNO₃, the mean size of AgNPs reached around 50 nm in another investigation [74]. Specific peaks in the XRD spectra were used to illustrate the XRD pattern of the AgNPs biosynthesized by *P. indica*. The face center cubic (fcc) nano-structures of AgNPs (111), (200), (220), (311), and (222), were characterized by five diffraction peaks at 2θ values of 38.2°, 44.46°, 64.22°, 77.52°, and 81.22°, respectively, with an average size 8–80 nm. According to another study, the diffraction peaks at $2\theta = 38.2^\circ, 46.2^\circ, 64.6^\circ,$ and 77.6° exemplify the 111, 200, 220, and 311 Bragg's reflection of Ag nanoparticles' face-centered-cubic structure [75]. Previous research that demonstrated the creation of AgNPs utilizing microbes had comparable XRD results [69,76,77].

Mucormycosis disease is very dangerous to humans and is caused by members of the Mucorales genera, such as *Rhizopus*, *Mucor*, and *Sycephalastrum*. Therefore, the control of these fungi by biomaterials is required. The biosynthesized AgNPs in this study revealed promising antifungal activity toward Mucorales genera species such as *R. microsporus*, *M. racemosus*, and *S. racemosum*. Medda et al. [78] synthesized AgNPs using Aloe vera leaf extract, and found antifungal activity toward *Rhizopus* sp. and *Aspergillus* sp. Alananbeh et al. [79] revealed that promising antifungal activity of AgNPs toward *M. hemalis* and *R. arrhizus*. AgNPs might be critical in breaking down such resistance. AgNPs' efficacy can be attributed to a variety of mechanisms, including cell wall disintegration, surface protein degradation, nucleic acid damage caused by the formation and buildup of reactive oxygen and nitrogen species (ROS and free radicals), and proton pump blocking. AgNPs are thought to cause a buildup of silver ions, which obstructs respiration by causing intracellular ion efflux, causing harm to the electron transport system [80].

Oxidative stress is a condition in which the balance between a cell's antioxidative defense and oxidants is disturbed as a result of oxidant excess [78]. Furthermore, the presence of oxidants causes oxidative changes of biological systems at the molecular level (unsaturated bonds of lipids, proteins, DNA, and so on), resulting in damage and, ultimately, hastened cellular death [79]. Antioxidants are natural or manmade compounds that can help to prevent or postpone oxidative cell damage (ROS, RNS, free radicals, other unstable molecules) [79]. Therefore, antioxidant compounds are continuously required to resist oxidative stress. The biosynthesized AgNPs in the current study revealed antioxidant activity where the IC₅₀ was 31 $\mu\text{g}/\text{mL}$. Previous studies have confirmed the antioxidant activity of AgNPs from different sources [81–83]. González-Ballesteros et al. [82] reported that AgNPs, silver nanoparticles, can be made from *Lactobacillus brevis* exopolysaccharides, and these were tested for antioxidant capabilities. At 100 g/mL , AgNPs had a moderate DPPH radical scavenging potential of 34.09% [83]. Evaluation of the cytotoxicity of compounds on human normal cell lines is considered the first step to detect their safety [64]. Therefore, the

cytotoxicity of biosynthesized AgNPs was assessed, where results confirmed that AgNPs are safe in use.

5. Conclusions

In the current study, a fast, green, eco-friendly method was used to synthesize AgNPs by *P. indica* S. Azhar for controlling fungi that cause mucormycosis, as well as antioxidant activity. Results revealed that AgNPs were fabricated using metabolites of *P. indica*, then, the biosynthesized AgNPs were characterized using different modern techniques. Moreover, the biosynthesized AgNPs exhibited outstanding antifungal activity against *R. microsporus*, *M. racemosus*, and *S. racemosum*. Furthermore, results revealed antioxidant activity without any cytotoxicity on the Vero normal cell line. The results of this study warrant further in vivo experiments.

Author Contributions: Conceptualization, S.S.S. and A.H.H.; methodology, S.S.S. and A.H.H.; validation, S.S.S. and A.H.H.; formal analysis, S.S.S. and A.H.H.; investigation, S.S.S., O.M.A., A.M.R., K.A.A.-E. and A.H.H.; software S.S.S. and A.H.H.; resources, S.S.S. and A.H.H.; data curation, S.S.S. and A.H.H.; Funding O.M.A. and K.A.A.-E.; writing—original draft preparation, S.S.S. and A.H.H.; writing—review and editing, S.S.S., O.M.A., A.M.R., K.A.A.-E. and A.H.H.; visualization, S.S.S., O.M.A., A.M.R., K.A.A.-E. and A.H.H. All authors have read and agreed to the published version of the manuscript.

Funding: This study was supported by the Taif University Researchers Supporting Project (TURSP-2020/81) at Taif University in Taif, Saudi Arabia.

Institutional Review Board Statement: Not applicable.

Informed Consent Statement: Not applicable.

Data Availability Statement: The data used to support the conclusions of this study are accessible upon request from the corresponding author.

Acknowledgments: The authors express their sincere thanks to Faculty of Science (Boys), Al-Azhar University, Cairo, Egypt for providing the necessary research facilities.

Conflicts of Interest: The authors declare that they have no conflict of interest.

References

1. Chang, Y.-L.; Yu, S.-J.; Heitman, J.; Wellington, M.; Chen, Y.-L. New facets of antifungal therapy. *Virulence* **2017**, *8*, 222–236. [[CrossRef](#)] [[PubMed](#)]
2. Campoy, S.; Adrio, J.L. Antifungals. *Biochem. Pharmacol.* **2017**, *133*, 86–96. [[CrossRef](#)] [[PubMed](#)]
3. Brown, G.D.; Denning, D.W.; Gow, N.A.; Levitz, S.M.; Netea, M.G. White TC (2012) Hidden killers: Human fungal infections. *Sci. Transl. Med.* **2012**, *4*, 165rv113. [[CrossRef](#)] [[PubMed](#)]
4. Kontoyiannis, D.P.; Lewis, R.E. Agents of mucormycosis and entomophthoromycosis. In *Mandell, Douglas, and Bennett's Principles and Practice of Infectious Diseases*; Elsevier: Amsterdam, The Netherlands, 2014; pp. 2909–2919.
5. Dacrory, S.; Hashem, A.H.; Hasanin, M. Synthesis of cellulose based amino acid functionalized nano-biocomplex: Characterization, antifungal activity, molecular docking and hemocompatibility. *Environ. Nanotechnol. Monit. Manag.* **2021**, *15*, 100453. [[CrossRef](#)]
6. Roden, M.M.; Zaoutis, T.E.; Buchanan, W.L.; Knudsen, T.A.; Sarkisova, T.A.; Schaufele, R.L.; Sein, M.; Sein, T.; Chiou, C.C.; Chu, J.H.; et al. Epidemiology and outcome of zygomycosis: A review of 929 reported cases. Clinical infectious diseases: An official publication of the Infectious Diseases Society of America. *Clin. Infect. Dis.* **2005**, *41*, 634–653. [[CrossRef](#)]
7. Petrikos, G.; Skiada, A.; Lortholary, O.; Roilides, E.; Walsh, T.J.; Kontoyiannis, D.P. Epidemiology and clinical manifestations of mucormycosis. Clinical infectious diseases: An official publication of the Infectious Diseases Society of America. *Clin. Infect. Dis.* **2012**, *54* (Suppl. 1), S23–S34. [[CrossRef](#)]
8. Walsh, T.J.; Gamaletsou, M.N.; McGinnis, M.R.; Hayden, R.T.; Kontoyiannis, D.P. Early clinical and laboratory diagnosis of invasive pulmonary, extrapulmonary, and disseminated mucormycosis (zygomycosis). Clinical infectious diseases: An official publication of the Infectious Diseases Society of America. *Clin. Infect. Dis.* **2012**, *54* (Suppl. 1), S55–S60. [[CrossRef](#)]
9. Skiada, A.; Lass-Floerl, C.; Klimko, N.; Ibrahim, A.; Roilides, E.; Petrikos, G. Challenges in the diagnosis and treatment of mucormycosis. *Med. Mycol.* **2018**, *56* (Suppl. 1), S93–S101. [[CrossRef](#)]
10. Sanglard, D.; Odds, F.C. Resistance of *Candida* species to antifungal agents: Molecular mechanisms and clinical consequences. *Lancet Infect. Dis.* **2002**, *2*, 73–85. [[CrossRef](#)]

11. Dannaoui, E. Antifungal resistance in mucorales. *Int. J. Antimicrob. Agents* **2017**, *50*, 617–621. [[CrossRef](#)]
12. Pfaller, M.A. Antifungal drug resistance: Mechanisms, epidemiology, and consequences for treatment. *Am. J. Med.* **2012**, *125*, S3–S13. [[CrossRef](#)] [[PubMed](#)]
13. Salem, S.S.; Fouda, A. Green Synthesis of Metallic Nanoparticles and Their Prospective Biotechnological Applications: An Overview. *Biol. Trace Elem. Res.* **2021**, *199*, 344–370. [[CrossRef](#)] [[PubMed](#)]
14. Shaheen, T.I.; Fouda, A.; Salem, S.S. Integration of Cotton Fabrics with Biosynthesized CuO Nanoparticles for Bactericidal Activity in the Terms of Their Cytotoxicity Assessment. *Ind. Eng. Chem. Res.* **2021**, *60*, 1553–1563. [[CrossRef](#)]
15. Fouda, A.; Salem, S.S.; Wassel, A.R.; Hamza, M.F.; Shaheen, T.I. Optimization of green biosynthesized visible light active CuO/ZnO nano-photocatalysts for the degradation of organic methylene blue dye. *Heliyon* **2020**, *6*, e04896. [[CrossRef](#)] [[PubMed](#)]
16. Salem, S.S.; Fouda, M.M.G.; Fouda, A.; Awad, M.A.; Al-Olayan, E.M.; Allam, A.A.; Shaheen, T.I. Antibacterial, Cytotoxicity and Larvicidal Activity of Green Synthesized Selenium Nanoparticles Using *Penicillium corylophilum*. *J. Clust. Sci.* **2021**, *32*, 351–361. [[CrossRef](#)]
17. Elfeky, A.S.; Salem, S.S.; Elzaref, A.S.; Owda, M.E.; Eladawy, H.A.; Saeed, A.M.; Awad, M.A.; Abou-Zeid, R.E.; Fouda, A. Multifunctional cellulose nanocrystal /metal oxide hybrid, photo-degradation, antibacterial and larvicidal activities. *Carbohydr. Polym.* **2020**, *230*, 115711. [[CrossRef](#)] [[PubMed](#)]
18. Sharaf, O.M.; Al-Gamal, M.S.; Ibrahim, G.A.; Dabiza, N.M.; Salem, S.S.; El-ssayad, M.F.; Youssef, A.M. Evaluation and characterization of some protective culture metabolites in free and nano-chitosan-loaded forms against common contaminants of Egyptian cheese. *Carbohydr. Polym.* **2019**, *223*, 115094. [[CrossRef](#)]
19. Hasanin, M.; Al Abboud, M.A.; Alawlaqi, M.M.; Abdelghany, T.M.; Hashem, A.H. Ecofriendly synthesis of biosynthesized copper nanoparticles with starch-based nanocomposite: Antimicrobial, antioxidant, and anticancer activities. *Biol. Trace Elem. Res.* **2021**, 1–14. [[CrossRef](#)]
20. Hasanin, M.; Hashem, A.H.; Lashin, I.; Hassan, S.A.M. In vitro improvement and rooting of banana plantlets using antifungal nanocomposite based on myco-synthesized copper oxide nanoparticles and starch. *Biomass Convers. Biorefin.* **2021**, 1–11. [[CrossRef](#)]
21. Hashem, A.H.; Khalil, A.M.A.; Reyad, A.M.; Salem, S.S. Biomedical Applications of Mycosynthesized Selenium Nanoparticles Using *Penicillium expansum* ATTC 36200. *Biol. Trace Elem. Res.* **2021**, *199*, 3998–4008. [[CrossRef](#)]
22. Eid, A.M.; Fouda, A.; Niedbała, G.; Hassan, S.E.D.; Salem, S.S.; Abdo, A.M.; Hetta, H.F.; Shaheen, T.I. Endophytic streptomyces laurentii mediated green synthesis of Ag-NPs with antibacterial and anticancer properties for developing functional textile fabric properties. *Antibiotics* **2020**, *9*, 641. [[CrossRef](#)] [[PubMed](#)]
23. Hashem, A.H.; Salem, S.S. Green and ecofriendly biosynthesis of selenium nanoparticles using *Urtica dioica* (stinging nettle) leaf extract: Antimicrobial and anticancer activity. *Biotechnol. J.* **2021**, 2100432. [[CrossRef](#)] [[PubMed](#)]
24. Badawy, A.A.; Abdelfattah, N.A.H.; Salem, S.S.; Awad, M.F.; Fouda, A. Efficacy assessment of biosynthesized copper oxide nanoparticles (CuO-nps) on stored grain insects and their impacts on morphological and physiological traits of wheat (*Triticum aestivum* L.) plant. *Biology* **2021**, *10*, 233. [[CrossRef](#)]
25. Mohamed, A.A.; Abu-Elghait, M.; Ahmed, N.E.; Salem, S.S. Eco-friendly Mycogenic Synthesis of ZnO and CuO Nanoparticles for In Vitro Antibacterial, Antibiofilm, and Antifungal Applications. *Biol. Trace Elem. Res.* **2021**, *199*, 2788–2799. [[CrossRef](#)]
26. Saied, E.; Eid, A.M.; Hassan, S.E.D.; Salem, S.S.; Radwan, A.A.; Halawa, M.; Saleh, F.M.; Saad, H.A.; Saied, E.M.; Fouda, A. The catalytic activity of biosynthesized magnesium oxide nanoparticles (Mgo-nps) for inhibiting the growth of pathogenic microbes, tanning effluent treatment, and chromium ion removal. *Catalysts* **2021**, *11*, 821. [[CrossRef](#)]
27. Abdelmoneim, H.E.M.; Wassel, M.A.; Elfeky, A.S.; Bendary, S.H.; Awad, M.A.; Salem, S.S.; Mahmoud, S.A. Multiple Applications of CdS/TiO₂ Nanocomposites Synthesized via Microwave-Assisted Sol–Gel. *J. Clust. Sci.* **2021**, 1–10. [[CrossRef](#)]
28. Hashem, A.H.; Abdelaziz, A.M.; Askar, A.A.; Fouda, H.M.; Khalil, A.M.A.; Abd-Elsalam, K.A.; Khaleil, M.M. *Bacillus megaterium*-Mediated Synthesis of Selenium Nanoparticles and Their Antifungal Activity against *Rhizoctonia solani* in Faba Bean Plants. *J. Fungi* **2021**, *7*, 195. [[CrossRef](#)]
29. Hashem, A.H.; Al Abboud, M.A.; Alawlaqi, M.M.; Abdelghany, T.M.; Hasanin, M. Synthesis of Nanocapsules Based on Biosynthesized Nickel Nanoparticles and Potato Starch: Antimicrobial, Antioxidant and Anticancer Activity. *Starch-Stärke* **2022**, *74*, 2100165. [[CrossRef](#)]
30. Mohamed, A.A.; Fouda, A.; Abdel-Rahman, M.A.; Hassan, S.E.-D.; El-Gamal, M.S.; Salem, S.S.; Shaheen, T.I. Fungal strain impacts the shape, bioactivity and multifunctional properties of green synthesized zinc oxide nanoparticles. *Biocatal. Agric. Biotechnol.* **2019**, *19*, 101103. [[CrossRef](#)]
31. Jain, N.; Jain, P.; Rajput, D.; Patil, U.K. Green synthesized plant-based silver nanoparticles: Therapeutic prospective for anticancer and antiviral activity. *Micro Nano Syst. Lett.* **2021**, *9*, 5. [[CrossRef](#)]
32. Abdel-Khalek, A.A.; Al-Quraishy, S.; Abdel-Gaber, R. Silver Nanoparticles Induce Time- and Tissue-Specific Genotoxicity in *Oreochromis niloticus*: Utilizing the Adsorptive Capacities of Fruit Peels to Minimize Genotoxicity. *Bull. Environ. Contam. Toxicol.* **2021**, 1–9. [[CrossRef](#)] [[PubMed](#)]
33. Nayak, S.; Manjunatha, K.B.; Goveas, L.C.; Rao, C.V.; Sajankila, S.P. Investigation of Nonlinear Optical Properties of AgNPs Synthesized Using *Cyclea peltata* Leaf Extract Post OVAT Optimization. *BioNanoScience* **2021**, *11*, 884–892. [[CrossRef](#)]

34. Beyene, H.D.; Werkneh, A.A.; Bezabh, H.K.; Ambaye, T.G. Synthesis paradigm and applications of silver nanoparticles (AgNPs), a review. *Sustain. Mater. Technol.* **2017**, *13*, 18–23. [[CrossRef](#)]
35. Elbahnasawy, M.A.; Shehabeldine, A.M.; Khattab, A.M.; Amin, B.H.; Hashem, A.H. Green biosynthesis of silver nanoparticles using novel endophytic *Rothia endophytica*: Characterization and anticandidal activity. *J. Drug Deliv. Sci. Technol.* **2021**, *62*, 102401. [[CrossRef](#)]
36. Hasanin, M.; Elbahnasawy, M.A.; Shehabeldine, A.M.; Hashem, A.H. Ecofriendly preparation of silver nanoparticles-based nanocomposite stabilized by polysaccharides with antibacterial, antifungal and antiviral activities. *BioMetals* **2021**, *34*, 1313–1328. [[CrossRef](#)]
37. Anees Ahmad, S.; Sachi Das, S.; Khatoon, A.; Tahir Ansari, M.; Afzal, M.; Saquib Hasnain, M.; Kumar Nayak, A. Bactericidal activity of silver nanoparticles: A mechanistic review. *Mater. Sci. Energy Technol.* **2020**, *3*, 756–769. [[CrossRef](#)]
38. Korkmaz, N.; Ceylan, Y.; Hamid, A.; Karadağ, A.; Bülbül, A.S.; Aftab, M.N.; Çevik, Ö.; Şen, F. Biogenic silver nanoparticles synthesized via *Mimusops elengi* fruit extract, a study on antibiofilm, antibacterial, and anticancer activities. *J. Drug Deliv. Sci. Technol.* **2020**, *59*, 101864. [[CrossRef](#)]
39. Pilaquinga, F.; Morey, J.; Torres, M.; Seqqat, R.; Piña, M.D.L.N. Silver nanoparticles as a potential treatment against SARS-CoV-2: A review. *WIREs Nanomed. Nanobiotechnol.* **2021**, *13*, e1707. [[CrossRef](#)]
40. Ciriminna, R.; Albo, Y.; Pagliaro, M. New Antivirals and Antibacterials Based on Silver Nanoparticles. *ChemMedChem* **2020**, *15*, 1619–1623. [[CrossRef](#)]
41. Bocate, K.P.; Reis, G.F.; de Souza, P.C.; Oliveira Junior, A.G.; Durán, N.; Nakazato, G.; Furlaneto, M.C.; de Almeida, R.S.; Panagio, L.A. Antifungal activity of silver nanoparticles and simvastatin against toxigenic species of *Aspergillus*. *Int. J. Food Microbiol.* **2019**, *291*, 79–86. [[CrossRef](#)]
42. Alam, A.; Tanveer, F.; Khalil, A.T.; Zohra, T.; Khamlich, S.; Alam, M.M.; Salman, M.; Ali, M.; Ikram, A.; Shinwari, Z.K.; et al. Silver nanoparticles biosynthesized from secondary metabolite producing marine actinobacteria and evaluation of their biomedical potential. *Antonie van Leeuwenhoek* **2021**, *114*, 1497–1516. [[CrossRef](#)] [[PubMed](#)]
43. Alomar, T.S.; AlMasoud, N.; Awad, M.A.; El-Tohamy, M.F.; Soliman, D.A. An eco-friendly plant-mediated synthesis of silver nanoparticles: Characterization, pharmaceutical and biomedical applications. *Mater. Chem. Phys.* **2020**, *249*, 123007. [[CrossRef](#)]
44. Shaheen, T.I.; Salem, S.S.; Fouda, A. Current Advances in Fungal Nanobiotechnology: Mycofabrication and Applications. In *Microbial Nanobiotechnology: Principles and Applications*; Lateef, A., Gueguim-Kana, E.B., Dasgupta, N., Ranjan, S., Eds.; Springer: Singapore, 2021; pp. 113–143. [[CrossRef](#)]
45. Aref, M.S.; Salem, S.S. Bio-callus synthesis of silver nanoparticles, characterization, and antibacterial activities via *Cinnamomum camphora* callus culture. *Biocatal. Agric. Biotechnol.* **2020**, *27*, 101689. [[CrossRef](#)]
46. Fouda, A.; Abdel-Maksoud, G.; Abdel-Rahman, M.A.; Salem, S.S.; Hassan, S.E.-D.; El-Sadany, M.A.-H. Eco-friendly approach utilizing green synthesized nanoparticles for paper conservation against microbes involved in biodeterioration of archaeological manuscript. *Int. Biodeterior. Biodegrad.* **2019**, *142*, 160–169. [[CrossRef](#)]
47. Huq, M.A. Green Synthesis of Silver Nanoparticles Using *Pseudoduganella eburnea* MAHUQ-39 and Their Antimicrobial Mechanisms Investigation against Drug Resistant Human Pathogens. *Int. J. Mol. Sci.* **2020**, *21*, 1510. [[CrossRef](#)] [[PubMed](#)]
48. Mohamed, A.A.; Fouda, A.; Elgamal, M.S.; EL-Din Hassan, S.; Shaheen, T.I.; Salem, S.S. Enhancing of cotton fabric antibacterial properties by silver nanoparticles synthesized by new Egyptian strain *Fusarium keratoplasticum* A1-3. In Proceedings of the 8th International Conference of The Textile Research Division (ICTRD 2017), National Research Centre, Cairo, Egypt, 25–27 September 2017; pp. 63–71.
49. Mohamed, A.A.; Saad, E.; Fouda, A.; Elgamal, M.S.; Salem, S.S. Extracellular biosynthesis of silver nanoparticles using *Aspergillus* sp. and evaluation of their antibacterial and cytotoxicity. *J. Appl. Life Sci. Int.* **2017**, *11*, 1–12. [[CrossRef](#)]
50. Tehri, N.; Vashishth, A.; Gahlaut, A.; Hooda, V. Biosynthesis, antimicrobial spectra and applications of silver nanoparticles: Current progress and future prospects. *Inorg. Nano-Met. Chem.* **2020**, *52*, 1–19. [[CrossRef](#)]
51. Zhang, D.; Ma, X.-L.; Gu, Y.; Huang, H.; Zhang, G.-W. Green Synthesis of Metallic Nanoparticles and Their Potential Applications to Treat Cancer. *Front. Chem.* **2020**, *8*, 799. [[CrossRef](#)] [[PubMed](#)]
52. Shehabeldine, A.M.; Hashem, A.H.; Wassel, A.R.; Hasanin, M. Antimicrobial and Antiviral Activities of Durable Cotton Fabrics Treated with Nanocomposite Based on Zinc Oxide Nanoparticles, Acyclovir, Nanochitosan, and Clove Oil. *Appl. Biochem. Biotechnol.* **2021**, 1–18. [[CrossRef](#)] [[PubMed](#)]
53. Iashin, I.; Hasanin, M.; Hassan, S.A.M.; Hashem, A.H. Green biosynthesis of zinc and selenium oxide nanoparticles using callus extract of *Ziziphus spina-christi*: Characterization, antimicrobial, and antioxidant activity. *Biomass Convers. Biorefin.* **2021**, 1–14. [[CrossRef](#)]
54. El-Naggar, M.E.; Hasanin, M.; Hashem, A.H. Eco-Friendly Synthesis of Superhydrophobic Antimicrobial Film Based on Cellulose Acetate/Polycaprolactone Loaded with the Green Biosynthesized Copper Nanoparticles for Food Packaging Application. *J. Polym. Environment.* **2021**, 1–13. [[CrossRef](#)]
55. Abd Elkodous, M.; El-Husseiny, H.M.; El-Sayyad, G.S.; Hashem, A.H.; Doghish, A.S.; Elfadil, D.; Radwan, Y.; El-Zeiny, H.M.; Bedair, H.; Ikhdair, O.A. Recent advances in waste-recycled nanomaterials for biomedical applications: Waste-to-wealth. *Nanotechnol. Rev.* **2021**, *10*, 1662–1739. [[CrossRef](#)]
56. Angelin, J.; Kavitha, M. Exopolysaccharides from probiotic bacteria and their health potential. *Int. J. Biol. Macromol.* **2020**, *162*, 853–865. [[CrossRef](#)] [[PubMed](#)]

57. Adetunji, A.I.; Olaniran, A.O. Production and potential biotechnological applications of microbial surfactants: An overview. *Saudi J. Biol. Sci.* **2021**, *28*, 669–679. [[CrossRef](#)] [[PubMed](#)]
58. Moreno, V.M.; Álvarez, E.; Izquierdo-Barba, I.; Baeza, A.; Serrano-López, J.; Vallet-Regí, M. Bacteria as Nanoparticles Carrier for Enhancing Penetration in a Tumoral Matrix Model. *Adv. Mater. Interfaces* **2020**, *7*, 1901942. [[CrossRef](#)] [[PubMed](#)]
59. Fouda, A.; Khalil, A.; El-Sheikh, H.; Abdel-Rhman, E.; Hashem, A. Biodegradation and detoxification of bisphenol-A by filamentous fungi screened from nature. *J. Adv. Biol. Biotechnol.* **2015**, *2*, 123–132. [[CrossRef](#)]
60. Hashem, A.H.; Hasanin, M.S.; Khalil, A.M.A.; Suleiman, W.B. Eco-green conversion of watermelon peels to single cell oils using a unique oleaginous fungus: *Lichtheimia corymbifera* AH13. *Waste Biomass Valoris.* **2019**, *11*, 5721–5732. [[CrossRef](#)]
61. Suleiman, W.; El-Sheikh, H.; Abu-Elreesh, G.; Hashem, A. Recruitment of *Cunninghamella echinulata* as an Egyptian isolate to produce unsaturated fatty acids. *Res. J. Pharm. Biol. Chem. Sci.* **2018**, *9*, 764–774.
62. Suleiman, W.; El-Sheikh, H.; Abu-Elreesh, G.; Hashem, A. Isolation and screening of promising oleaginous *Rhizopus* sp. and designing of Taguchi method for increasing lipid production. *J. Innov. Pharm. Biol. Sci.* **2018**, *5*, 8–15.
63. Rodriguez-Tudela, J.; Arendrup, M.; Arikian, S.; Barchiesi, F.; Bille, J.; Chryssanthou, E.; Cuenca-Estrella, M.; Dannaoui, E.; Denning, D.; Donnelly, J. Eucast Definitive Document E. Def 9.1: Method for the determination of broth dilution minimum inhibitory concentrations of antifungal agents for conidia forming moulds. *Def* **2008**, *9*, 1–13.
64. Khalil, A.; Abdelaziz, A.; Khaleil, M.; Hashem, A. Fungal endophytes from leaves of *Avicennia marina* growing in semi-arid environment as a promising source for bioactive compounds. *Let. Appl. Microbiol.* **2021**, *72*, 263–274. [[CrossRef](#)] [[PubMed](#)]
65. Van de Loosdrecht, A.; Beelen, R.; Ossenkoppele, G.; Broekhoven, M.; Langenhuijsen, M. A tetrazolium-based colorimetric MTT assay to quantitate human monocyte mediated cytotoxicity against leukemic cells from cell lines and patients with acute myeloid leukemia. *J. Immunol. Methods* **1994**, *174*, 311–320. [[CrossRef](#)]
66. Ioset, J.-R.; Brun, R.; Wenzler, T.; Kaiser, M.; Yardley, V. *Drug Screening for Kinetoplastids Diseases: A Training Manual for Screening in Neglected Diseases*; DNDi and Pan-Asian Screening Network: Geneva, Switzerland, 2009.
67. Wypij, M.; Czarnecka, J.; Świecimska, M.; Dahm, H.; Rai, M.; Golinska, P. Synthesis, characterization and evaluation of antimicrobial and cytotoxic activities of biogenic silver nanoparticles synthesized from *Streptomyces xinghaiensis* OF1 strain. *World J. Microbiol. Biotechnol.* **2018**, *34*, 23. [[CrossRef](#)] [[PubMed](#)]
68. Alsharif, S.M.; Salem, S.S.; Abdel-Rahman, M.A.; Fouda, A.; Eid, A.M.; Hassan, S.E.D.; Awad, M.A.; Mohamed, A.A. Multi-functional properties of spherical silver nanoparticles fabricated by different microbial taxa. *Heliyon* **2020**, *6*, e03943. [[CrossRef](#)] [[PubMed](#)]
69. Salem, S.S.; El-Belely, E.F.; Niedbała, G.; Alnoman, M.M.; Hassan, S.E.D.; Eid, A.M.; Shaheen, T.I.; Elkesh, A.; Fouda, A. Bactericidal and in-vitro cytotoxic efficacy of silver nanoparticles (Ag-NPs) fabricated by endophytic actinomycetes and their use as coating for the textile fabrics. *Nanomaterials* **2020**, *10*, 2082. [[CrossRef](#)]
70. Alsamhary, K.I. Eco-friendly synthesis of silver nanoparticles by *Bacillus subtilis* and their antibacterial activity. *Saudi J. Biol. Sci.* **2020**, *27*, 2185–2191. [[CrossRef](#)]
71. Saeed, S.; Iqbal, A.; Ashraf, M.A. Bacterial-mediated synthesis of silver nanoparticles and their significant effect against pathogens. *Environ. Sci. Pollut. Res.* **2020**, *27*, 37347–37356. [[CrossRef](#)]
72. Ibrahim, E.; Zhang, M.; Zhang, Y.; Hossain, A.; Qiu, W.; Chen, Y.; Wang, Y.; Wu, W.; Sun, G.; Li, B. Green-Synthesization of Silver Nanoparticles Using Endophytic Bacteria Isolated from Garlic and Its Antifungal Activity against Wheat Fusarium Head Blight Pathogen *Fusarium graminearum*. *Nanomaterials* **2020**, *10*, 219. [[CrossRef](#)]
73. Sarangadharan, S.; Nallusamy, S. Biosynthesis and characterization of silver nanoparticles produced by *Bacillus licheniformis*. *Int. J. Pharma Med. Biol. Sci.* **2015**, *4*, 236.
74. Kalimuthu, K.; Babu, R.S.; Venkataraman, D.; Bilal, M.; Gurunathan, S. Biosynthesis of silver nanocrystals by *Bacillus licheniformis*. *Colloids Surf. B Biointerfaces* **2008**, *65*, 150–153. [[CrossRef](#)]
75. Fouad, H.; Hongjie, L.; Yanmei, D.; Baoting, Y.; El-Shakh, A.; Abbas, G.; Jianchu, M. Synthesis and characterization of silver nanoparticles using *Bacillus amyloliquefaciens* and *Bacillus subtilis* to control filarial vector *Culex pipiens pallens* and its antimicrobial activity. *Artif. Cells Nanomed. Biotechnol.* **2017**, *45*, 1369–1378. [[CrossRef](#)] [[PubMed](#)]
76. Du, J.; Singh, H.; Yi, T.-H. Biosynthesis of silver nanoparticles by *Novosphingobium* sp. THG-C3 and their antimicrobial potential. *Artif. Cells Nanomed. Biotechnol.* **2017**, *45*, 211–217. [[CrossRef](#)] [[PubMed](#)]
77. Zonooz, N.F.; Salouti, M. Extracellular biosynthesis of silver nanoparticles using cell filtrate of *Streptomyces* sp. ERI-3. *Scientia Iranica* **2011**, *18*, 1631–1635. [[CrossRef](#)]
78. Medda, S.; Hajra, A.; Dey, U.; Bose, P.; Mondal, N.K. Biosynthesis of silver nanoparticles from Aloe vera leaf extract and antifungal activity against *Rhizopus* sp. and *Aspergillus* sp. *Appl. Nanosci.* **2015**, *5*, 875–880. [[CrossRef](#)]
79. Alananbeh, K.; Al-Refae, W.; Al-Qodah, Z. Antifungal effect of silver nanoparticles on selected fungi isolated from raw and waste water. *Indian J. Pharm. Sci.* **2017**, *79*, 559–567. [[CrossRef](#)]
80. Du, H.; Lo, T.-M.; Sitompul, J.; Chang, M.W. Systems-level analysis of *Escherichia coli* response to silver nanoparticles: The roles of anaerobic respiration in microbial resistance. *Biochem. Biophys. Res. Commun.* **2012**, *424*, 657–662. [[CrossRef](#)] [[PubMed](#)]
81. Azeez, L.; Lateef, A.; Adebisi, S.A. Silver nanoparticles (AgNPs) biosynthesized using pod extract of *Cola nitida* enhances antioxidant activity and phytochemical composition of *Amaranthus caudatus* Linn. *Appl. Nanosci.* **2017**, *7*, 59–66. [[CrossRef](#)]

82. González-Ballesteros, N.; Rodríguez-Argüelles, M.C.; Prado-López, S.; Lastra, M.; Grimaldi, M.; Cavazza, A.; Nasi, L.; Salviati, G.; Bigi, F. Macroalgae to nanoparticles: Study of *Ulva lactuca* L. role in biosynthesis of gold and silver nanoparticles and of their cytotoxicity on colon cancer cell lines. *Mater. Sci. Eng. C* **2019**, *97*, 498–509. [[CrossRef](#)]
83. Patra, J.K.; Baek, K.-H. Antibacterial Activity and Synergistic Antibacterial Potential of Biosynthesized Silver Nanoparticles against Foodborne Pathogenic Bacteria along with its Anticandidal and Antioxidant Effects. *Front. Microbiol.* **2017**, *8*, 167. [[CrossRef](#)]